Snail-overexpressing Cancer Cells Promote M2-Like Polarization of Tumor-Associated Macrophages by Delivering MiR-21-Abundant Exosomes

Chia-Hsin Hsieh[†], Shyh-Kuan Tai[¶] and Muh-Hwa Yang[*,†,‡,§]

[*]Institute of Clinical Medicine, National Yang-Ming University, Taipei 11221, Taiwan; [†]Biotechnology and Laboratory Science in Medicine, National Yang-Ming University, Taipei 11221, Taiwan; [‡]Cancer Progression Research Center, National Yang-Ming University, Taipei 11221, Taiwan; [§]Division of Medical Oncology, Department of Oncology, Taipei Veterans General Hospital, Taipei 11217, Taiwan; [¶]Department of Otolaryngology, Taipei Veterans General Hospital, Taipei 11217, Taiwan

Abstract

Epithelial-mesenchymal transition (EMT) is a major event during cancer progression and metastasis; however, the definitive role of EMT in remodeling tumor microenvironments (TMEs) is unclear. Tumor-associated macrophages (TAMs) are a major type of host immune cells in TMEs, and they perform a wide range of functions to regulate tumor colonization and progression by regulating tumor invasiveness, local tumor immunity, and angiogenesis. TAMs are considered to have an M2-like, i.e., alternatively activated, phenotype; however, how these EMT-undergoing cancer cells promote M2 polarization of TAMs as a crucial tumor-host interplay during cancer progression is unclear. In this study, we investigated the mechanism of EMT-mediated TAM activation. Here, we demonstrate that the EMT transcriptional factor Snail directly activates the transcription of *MIR21* to produce miR-21-abundant tumor-derived exosomes (TEXs). The miR-21-containing exosomes were engulfed by CD14$^+$ human monocytes, suppressing the expression of M1 markers and increasing that of M2 markers. Knockdown of miR-21 in Snail-expressing human head and neck cancer cells attenuated the Snail-induced M2 polarization, angiogenesis, and tumor growth. In head and neck cancer samples, a high expression of miR-21 was correlated with a higher level of *SNAI1* and the M2 marker *MRC1*. This study elucidates the mechanism of EMT-mediated M2 polarization through delivery of the miR-21-abundant exosomes, which may serve as a candidate biomarker of tumor progression and provide a potential target for intercepting EMT-mediated TME remodeling.

Neoplasia (2018) 20, 775–788

Introduction

Tumor microenvironments (TMEs) contain the cellular and non-cellular components that closely interact with tumor cells to influence tumor growth, progression and metastasis. A key element of the TME is the host immune system that is composed of the major effector cells of the innate/adaptive immune system [1]. Among these, tumor-associated macrophages (TAMs) are the most abundant innate immune cells in the TME, and they play crucial roles in tumor progression [2]. In physiological environments, macrophages can be categorized into classically activated (M1) macrophages, which produce pro-inflammatory cytokines to exert the host-defense function [3], and alternatively activated (M2) macrophages that secrete anti-inflammatory cytokines for tissue regeneration and
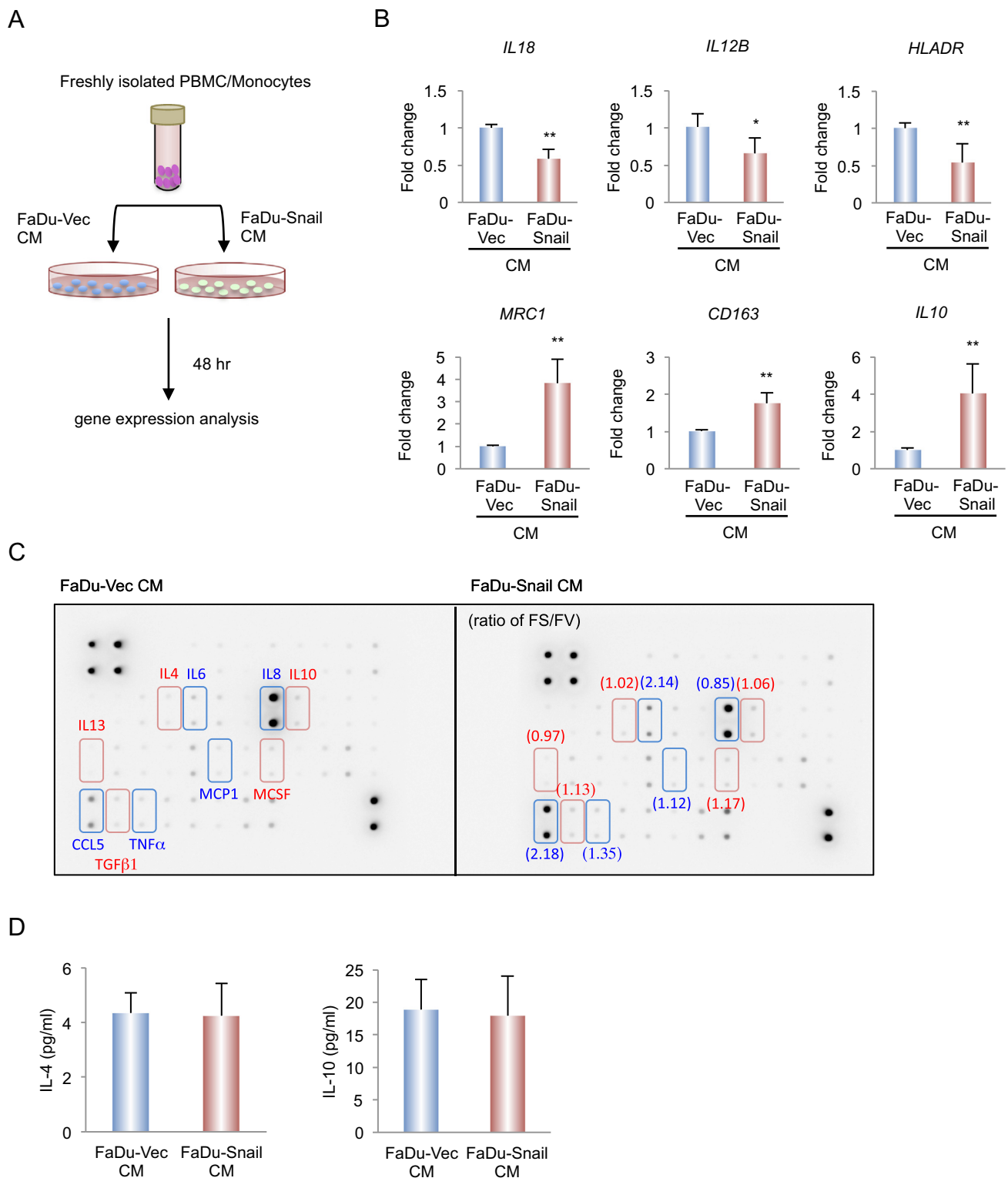
Figure 1. Snail-expressing cancer cells promotes M2-like polarization of macrophages. (A) Schema for representing the experiment procedure. (B) RT-qPCR for analyzing the expression of the markers of M1 (*IL18*, *IL12B*, *HLADR*) and M2 (*MRC1*, *CD163*, *IL10*) macrophages in CD14$^+$ human monocytes incubated with the conditioned medium from FaDu-Vec/FaDu-Snail for 48 hr. Data represents means ± S.D. * *P* < .05, ** *P* < .005 by Student's *t*-test. n = 3 independent experiments (each experiment contains 2 technical replicates). CM, conditional media. (C) Analysis of the conditioned media secreted by FaDu-Vec (left)/FaDu-Snail (right) by cytokine array. Blue, M1-promoting cytokines; red, M2-promoting cytokines. The ratio of FaDu-Snail/FaDu-Vec of the cytokines is shown in the right panel. CM, conditioned media. (D) ELISA for analyzing IL-4 and IL-10 from the conditional media of FaDu-Snail/FaDu-Vec cells. n = 3 independent experiments (each experiment contains 2 technical replicates). CM, conditioned media.

immunosuppression [4]. In contrast, TAMs often exhibit an M2-like phenotype to facilitate tumor progression by promoting angiogenesis, tumor cell proliferation, and tumor metastasis [5]. TAMs primarily

originate from the recruited monocytes, which differentiate and activate into macrophages in response to various factors produced by the cells residing in the TME, such as stromal cells, T cells and
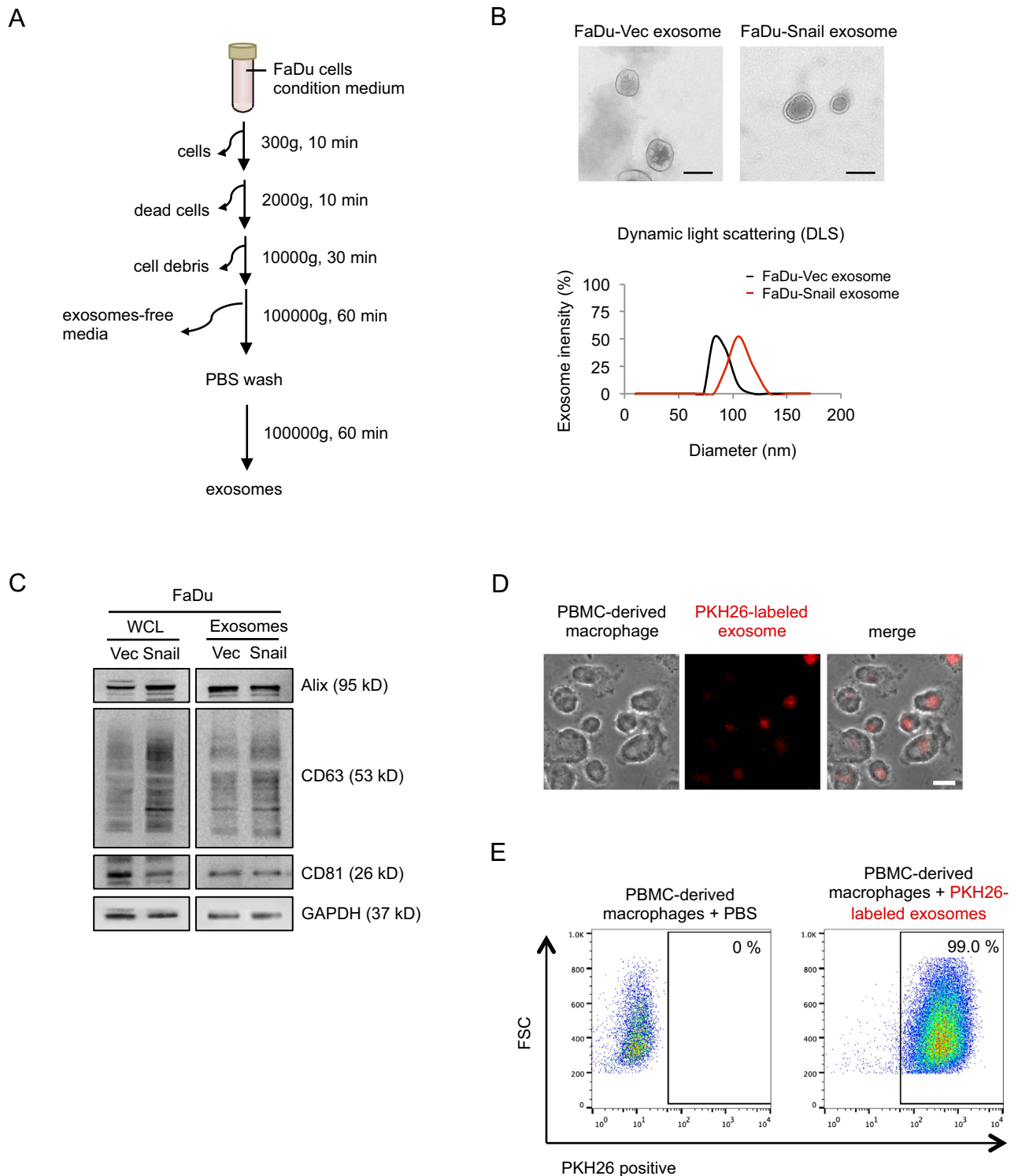

Figure 2. Isolation and characterization of tumor-derived exosomes. (A) Flow chart for illustrating the procedures of exosomes purification through ultracentrifugation. (B) Upper: representative photos of FaDu-Snail/FaDu-Vec-secreted exosomes with the lipid-bilayer structure by TEM transmission electron-microscopy. Lower, size distribution of exosomes analyzed by DLS (dynamic light scattering). Scale bar, 100 nm. (C) Western blot analysis of the expression of exosome markers (CD63, CD81, Alix) in whole cell lysates (WCL) and exosomes derived from FaDu-Vec and FaDu-Snail cells. GAPDH was used as a loading control. (D) The representative phase-contrast images of peripheral blood mononuclear cells (PBMC)-derived macrophages (left) incubated with PKH26-labeled exosomes (middle) for 24 hr. The merged image is shown at the right panel. Scale bar, 20 μm. (E) Flow cytometry for analyzing the percentage of PKH26-labeled exosomes engulfed by PBMC-derived macrophage when co-incubated for 24 hr.
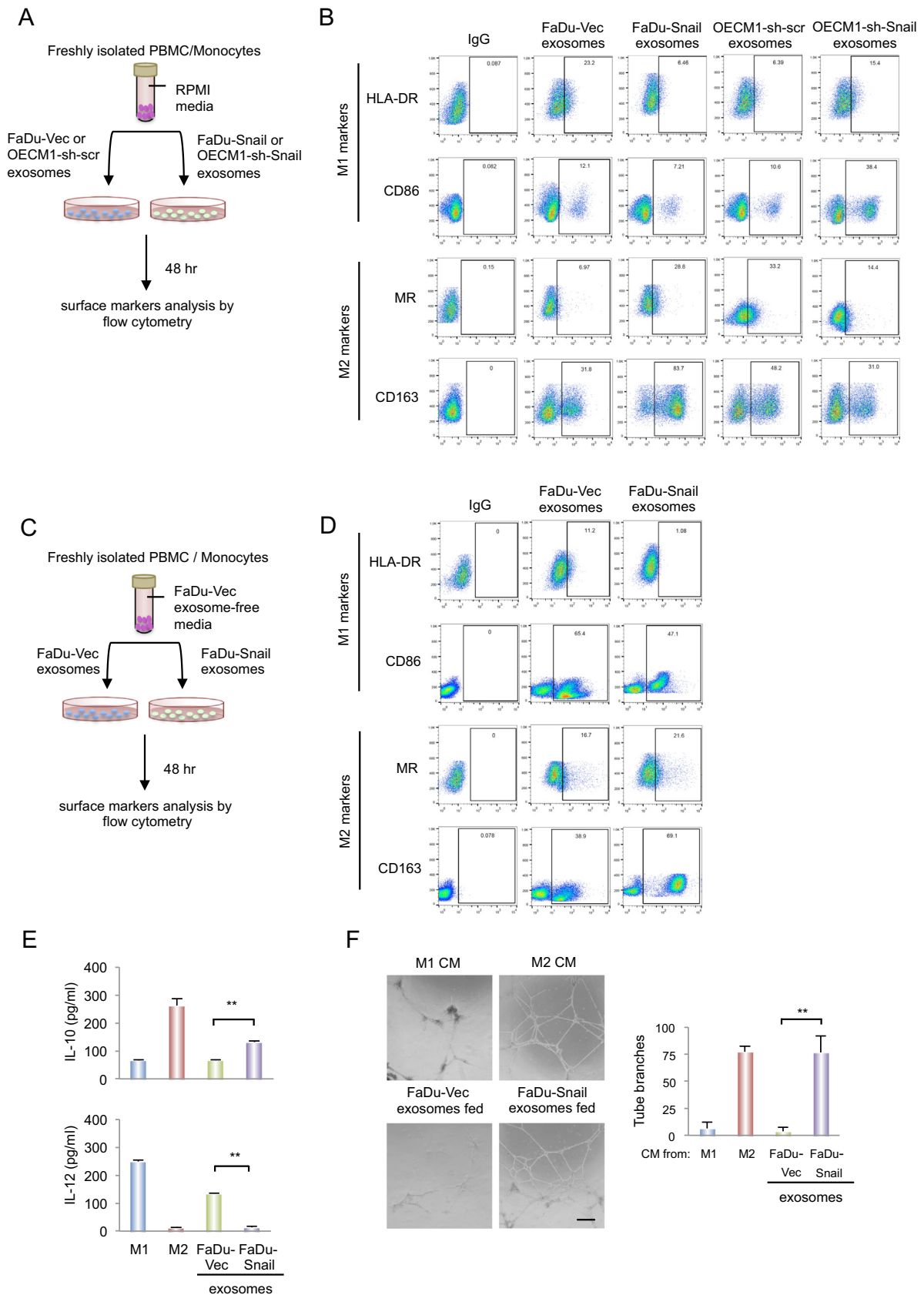
tumor cells [6]. The factors responsible for the recruitment and activation of TAMs are chiefly cytokines/chemokines/growth factors [7-9]. In addition to the secreted proteins, emerging evidence supports the role of cancer-secreted extracellular vesicles in modulating the TME, including macrophage activation [10]. Although the interplay between tumor cells and macrophages has been firmly established, the understanding of cancer-directed signals for guiding this communication to modulate the TME is relatively limited.

Exosomes are extracellular vesicles with a diameter of 30 to 100 nm and are secreted by different types of cells to serve as functional mediators for regulating various physiological and pathological processes [11]. The major contents of exosomes include cytosolic/transmembrane proteins, lipids, microRNAs (miRNAs), long non-coding mRNAs (lncRNAs), and DNA [12-14]. Recent studies have highlighted the role of tumor-derived exosomes (TEXs) in the TME in cancer progression through modulation of the interaction between tumor cells and stroma. The major functions of TEXs include tumor-mediated immunosuppression, angiogenesis, and pre-metastatic niche formation. For immunosuppression, TEXs that express Fas ligands induce apoptosis of T cells [15]; TEXs skew the responsiveness of IL-2 in favor of regulatory T cells and away from cytotoxic cells through delivering membrane-associated TGFβ1 [16]. TEXs from hypoxic conditions accelerate GBM tumor growth and angiogenesis [17]. Pancreatic cancer TEXs internalized by Kupffer cells cause TGFβ secretion, fibronectin production and liver pre-metastatic niche formation [18]; breast cancer-derived exosomes accumulate Dicer to process pre-miRNAs into mature miRNAs in exosomes, thus facilitating tumor formation [19]. Nevertheless, it is unclear whether TEXs are a major route for cancer-mediated TAM polarization/activation.

Cancer progression is a series of complicated processes, which include the evolution of cancer cells to harbor the metastatic potential and remodeling of microenvironments. Epithelial-mesenchymal transition (EMT) is a major event for regulating epithelial plasticity to ensure cancer progression. Accumulating evidence suggests that EMT is involved in tumor-host interplay beyond cytoskeletal remodeling [20,21]. We recently demonstrated that the EMT transcriptional factor (EMT-TF) Snail activates the expression of different cytokines such as IL-6, IL-8, CCL2, and CCL5 in cancer cells to promote the recruitment of TAMs. Intriguingly, we also noted that Snail-expressing cancer cells not only are able to recruit TAMs but also promote M2-like polarization [22]. However, the major cytokines secreted by the Snail-expressing cells are not the canonical cytokines that induce alternative activation of macrophages, and the potential mechanism responsible for Snail-mediated M2

polarization is elusive. Importantly, the role of EMT in inducing M2 activation to facilitate cancer progression is unclear. In this study, we demonstrate that Snail induces the expression of miR-21 through transcriptional activation. Secretion of miR-21-abundant exosomes from cancer cells suppresses the expression of target genes such as *PDCD4* and *IL12A* and promotes M2-like polarization of macrophages. This observation highlights the role of TEXs from EMT-undergoing cancer cells in modulating the TME, indicating candidate targets for combating progressive tumors.

Material and Methods

Cell Lines and Plasmids

The human head and neck squamous cell carcinoma (HNSCC) cell line FaDu and the human embryonic kidney cell line 293T were originally obtained from American Type Culture Collection (ATCC). The HNSCC cell line OEC-M1 was obtained from Dr. Kuo-Wei Chang (National Yang-Ming University of Taiwan). The pCDH-Snail plasmid was generated by inserting full-length cDNA (SNAI1: NM_005985) into the pCDH-CMV-MCS-EF1-puro vector. The pLKO.1-scramble (ASN0000000004) and *SNAI1* shRNA (TRCN0000063818) were obtained from the National RNAi Core Facility of Taiwan for gene silencing. The miRZip anti-miR-21 (MZIP21-PA-1) was purchased from System BioSciences (Palo Alto, CA). The promoter region of *MIR21*, which was defined according to a previous report [23], was cloned into pGL4.2 to generate LucA and LucB, and site-directed mutagenesis was applied to generate the E-box-mutated 1216+ 856 mut.

Preparation of Conditioned Media of Cancer Cells and Cytokine Array Analysis

To produce conditioned media from cancer cells, the cancer cell line FaDu with ectopic expression of Snail/control vector (FaDu-Snail/FaDu-Vec) was cultivated in RPMI growth media supplemented with penicillin/streptomycin and 0.5% FBS for 48 hr. The supernatant was centrifuged at 2000 × g for 5 min and then collected and stored at –80 °C. For detecting the expression of multiple cytokines secreted from FaDu-Snail/FaDu-Vec, the conditioned media were analyzed by cytokine array (AAH-INF-3-4, RayBiotech, Inc., Norcross, GA).

Purification and Characterization of Tumor-Derived Exosomes

Exosome purification was performed as described previously [24]. Briefly, exosomes were purified by differential ultracentrifugation. The cells were cultured in media supplemented with 10% exosome-

Figure 3. Snail-expressing cancer cells promotes M2-like polarization of macrophages through delivering exosomes. (A) Schema for representing the experiment procedures of (B). (B) Flow cytometry for analyzing the expression of HLA-DR, CD86, MR, and CD163 in CD14+ human monocytes incubated with the exosomes derived from FaDu-Vec/FaDu-Snail or OECM1-sh-scr/OECM1-sh-Snail for 48 hr. (C) Schema for representing the experiment procedure of (D). (D) Flow cytometry for analyzing the expression of HLA-DR, CD86, MR, and CD163 in CD14+ human monocytes incubated with the exosome-free conditioned media from FaDu-Vec mixed with the exosomes isolated from FaDu-Vec/FaDu-Snail for 48 hr. (E) ELISA for analyzing the secretion of IL-10 and IL-12 in FaDu-Snail/FaDu-Vec exosomes incubated CD14+ monocytes for 48 hr. The in vitro polarized M1/M2 macrophages were used as a control of the experiment. Data represents means ± S.D. ** $P <$ .005 by Student's t-test. n = 3 independent experiments (each experiment contains 2 technical replicates).(F) Tube formation assay. Human Umbilical Vein Endothelial Cells (HUVECs) were incubated with the supernatants from CD14+ human monocytes fed with the FaDu-Vec/FaDu-Snail-secreted exosomes for 48 hr. M1 and M2 conditioned media were used as the control of the experiment. Left: representative photos. Scale bar, 50 μm. Right: quantification of the results. Data represents means ± S.D. n = 3 independent experiments. ** $P <$ .005 by Student's t-test.

depleted FBS (ultracentrifuged at 100,000 × g for 120 min) for 48 hr. The cells were removed from the conditioned media by centrifugation at 300 × g for 10 min. To remove the dead cells and cell debris, the supernatants were successively centrifuged at increasing speeds (2000 × g for 10 min, 10,000 × g for 30 min,

Beckman SW28 rotor). Next, the supernatant was then ultracentrifuged at 100,000 × g for 60 min to pellet the exosomes. The exosomes were washed in PBS and centrifuged one last time at the same high speed (Beckman TLA-100.3 rotor). The morphology and size distribution of the exosomes were analyzed by transmission
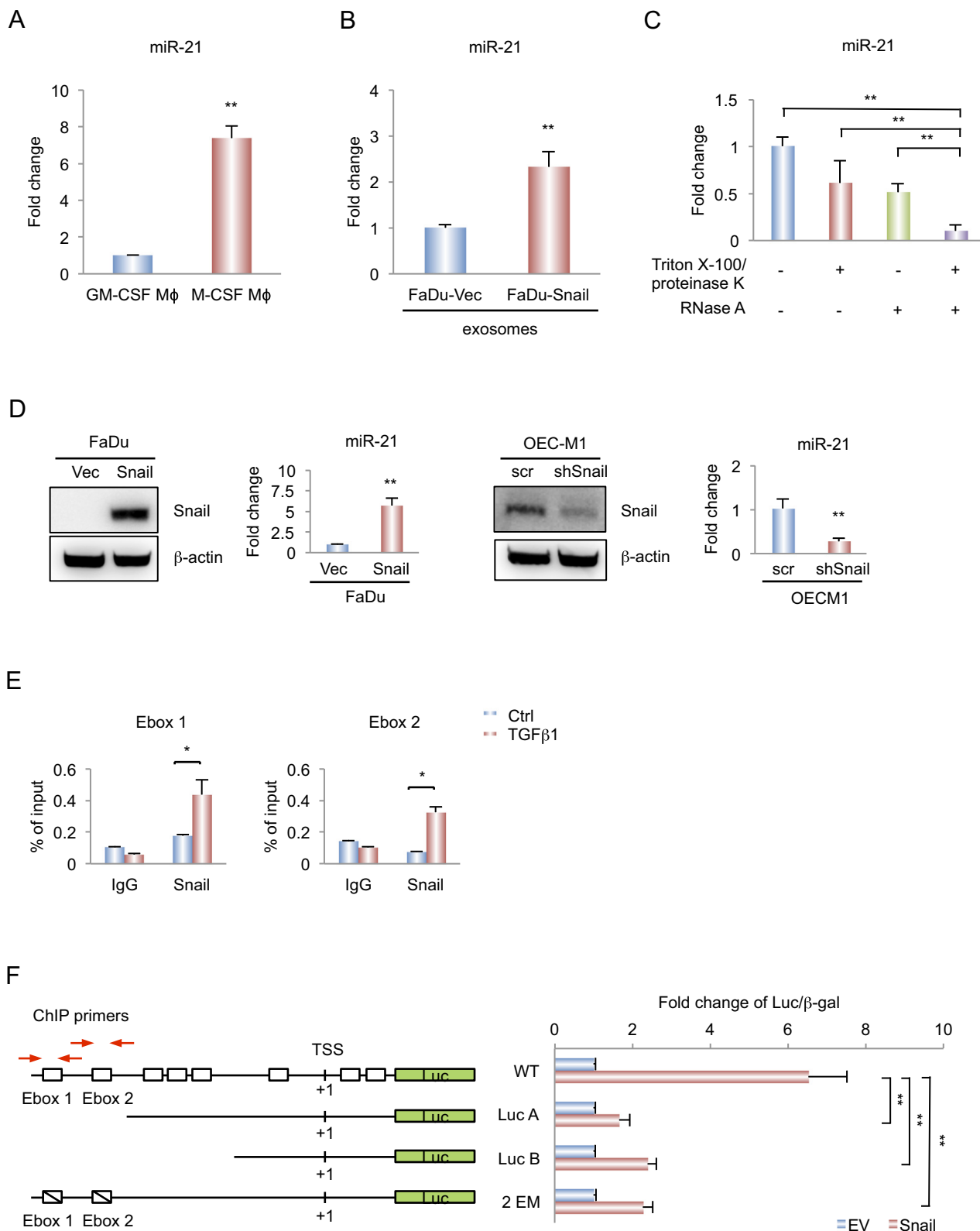
electron-microscopy (JEOL JEM-2000EXII, JEOL USA, Inc., Peabody, MA) and dynamic light scattering (DLS; Zetasizer Nano ZS90, Worcestershire, UK), respectively. To confirm the engulfment of exosomes by macrophages, the peripheral blood mononuclear cell (PBMC)-derived macrophages were incubated with PKH26-labeled exosomes for 24 hr. Images were collected sequentially on a confocal laser scanning microscope (Olympus UPLSAPO 60XO, NA 1.35) and analyzed by Olympus FV10-ASW Version 3.0 Software. The engulfment of PKH26-labeled exosomes by macrophages was validated by flow cytometric analysis.

Preparation of Human Monocytes and Treatment

Mononuclear cells were isolated from human whole blood by standard density gradient centrifugation with Ficoll-Paque (Amersham Biosciences, Inc., Piscataway, NJ). CD14$^+$ cells were subsequently purified from the peripheral mononuclear cells by high-gradient magnetic sorting using anti-CD14 microbeads (No. 130–050-201, Miltenyi Biotec GmbH, Bergisch Gladbach, Germany). For preparation of human PBMC-derived macrophages, the CD14$^+$ cells were cultured in RPMI media containing 10% FBS and 20 ng/ml GM-CSF or M-CSF for 5 days to establish macrophages. After polarization, the macrophages were cultured in FaDu-Snail/FaDu-Vec conditioned media or incubated with 30 μg/ml exosomes derived from FaDu-Snail/FaDu-Vec for 48 hr.

Animal Experiments

The animal experiment was approved by the Institutional Animal Care and Utilization Committee of Taipei Veterans General Hospital (IACUC certificate No. 2013–169). The animal experiments include three parts. The first part is the orthotopic implantation assay in which 2x10^5 FaDu cells expressing a control vector or Snail with/without knockdown of miR-21 were injected into the tongue of BALB/c nude mice (n = 5 or 6, Figure 5A-C). The mice were sacrificed on the 24th day after the tumor cell injections, and the orthotopic tumors were harvested for measuring Snail expression, TAM infiltration and microvascular densities. The second experiment was performed by inoculating 1x10^6 FaDu cells expressing a control vector or Snail with/without knockdown of miR-21 into the subcutaneous area of the BALB/c nude mice (n = 5 for each group, Figure 5D-F). The size of the tumor was measured regularly. In the third experiment, FaDu-Vec/FaDu-Snail cells co-expressed with Flag-

tagged CD81 were implanted into the BALB/c nude mice (n = 5 for each group, Figure S4B and C). The mice were sacrificed on the 14th day after tumor cell inoculation. The tumors were harvested, and tumor-infiltrating CD11b$^+$F4/80$^+$ cells were isolated by BD FACSAria (BD Biosciences, Franklin Lakes, NJ). The CD11b$^+$F4/80$^+$ cells were stained with Flag antibody for 16 hr. at 4 °C and then with secondary FITC-conjugated goat anti-mouse IgG antibody for 1 hr. at 4 °C. The images were captured using an Olympus Fluoview FV10i Laser confocal microscope (Olympus Corporation, Tokyo, Japan) equipped with a 60x oil objective (Olympus UPLSAPO 60XO, NA 1.35) and analyzed by Olympus FV10-ASW Version 3.0 Software.

Immunoblotting

These procedures were performed as previously described [22]. The results were measured using a GE LAS-4000 (GE Healthcare Inc., Marlborough, MA). Information about the antibodies used in the experiments is listed in Supplementary Table 2.

RNA Extraction, Reverse Transcription, and Quantitative PCR Analysis

To analyze the amounts of different transcripts, total RNAs from the cultured cells were extracted using the Trizol reagent (Invitrogen Life Technologies, Waltham, MA), and 1 μg of RNA was used for cDNA synthesis. Quantitative PCR was performed using the StepOnePlus real-time PCR system (Applied Biosystems Inc., Foster City, CA). The primer sequences used for real-time PCR are listed in Supplementary Table 3.

Flow Cytometry

The cells were harvested, washed twice with PBS, incubated with primary antibodies (see Supplementary Table 2) for 1 hr. at 4 °C and then incubated with secondary antibodies for 30 min at 4 °C. The stained cells were analyzed on a BD FACSCalibur™ system (BDBiosciences, Franklin Lakes, NJ) using CELLQuest Analysis software (BDBiosciences, Franklin Lakes, NJ) and FlowJo software (FlowJo LLC, Ashland, OR, USA).

Enzyme-Linked Immunosorbent Assay (ELISA)

The amount of cytokines were determined using ELISA kits for detecting human IL-4 (BMS225INST, eBioscience, Inc., San Diego, CA), IL-10 (BMS215INST, eBioscience, Inc., San Diego, CA) and

---

Figure 4. Enrichment of miR-21 in Snail-expressed cancer cells and Snail activates *MIR21* transcription. (A) RT-qPCR for analyzing the expression of miR-21 in CD14$^+$ monocytes treated with 20 ng/ml GM-CSF or M-CSF for 5 days. Data represent means ± S.D. ** $P <$ .005 by Student's *t*-test. n = 3 independent experiments (each experiment contains 2 technical replicates). (B) RT-qPCR for analyzing the expression of miR-21 in CD14$^+$ human monocytes incubated with the exosomes derived from the supernatant of FaDu-Vec or FaDu-Snail cultivated in RPMI medium for 48 hr. Data represent means ± S.D. ** $P <$ .005 by Student's t-test. n = 3 independent experiments (each experiment contains 2 technical replicates). (C) RT-qPCR for analyzing the expression of miR-21 in exosomes derived from FaDu-Snail in the presence or absence of Triton X-100/proteinase K or RNase A. Data represent means ± S.D. ** $P <$ .005 by Student's *t*-test. n = 3 independent experiments (each experiment contains 2 technical replicates). (D) Western blot of Snail and RT-qPCR of miR-21 in FaDu-Vec/FaDu-Snail and OEC-M1 cells receiving shRNA against Snail (OECM1-shSnail)/a control sequence (OECM1-scr). β-actin was used as a loading control for immunoblots. For RT-qPCR, data represent means ± S.D. ** $P <$ .005 by Student's *t*-test. n = 3 independent experiments (each experiment contains 2 technical replicates). (E) Quantitative ChIP in FaDu cells stimulated with or without 5 ng/ml TGFβ1 for 7 days. The protein-DNA was crosslinked and immunoprecipitated by an anti-Snail antibody, and IgG was a control for immunoprecipitation. The DNA fragments containing the Snail binding sites on the promoter of *MIR21* were amplified by quantitative PCR and presented as the percentage of input. Data represent means ± S.D. * $P <$ .05 by Student's *t*-test. n = 3 independent experiments (each experiment contains 2 technical replicates). (F) Left, schematic representation of the promoter region of *MIR21* gene and reporter constructs used in HEK293T cells transient transfection. The primers for amplifying the regions in ChIP experiments (E) are also indicated. The constructs were wild-type (WT), E-box deleted (Luc A and Luc B), or E-box mutated (2EM). HEK293T cells were co-transfected with the indicated promoter construct and Snail or empty vector (EV). The results are presented as the fold changes of luciferase activity/β-galactosidase (β-gal). Data represent means ± S.D. ** P < .005 by Student's *t*-test. n = 3 independent experiments (each experiment contains 2 technical replicates).
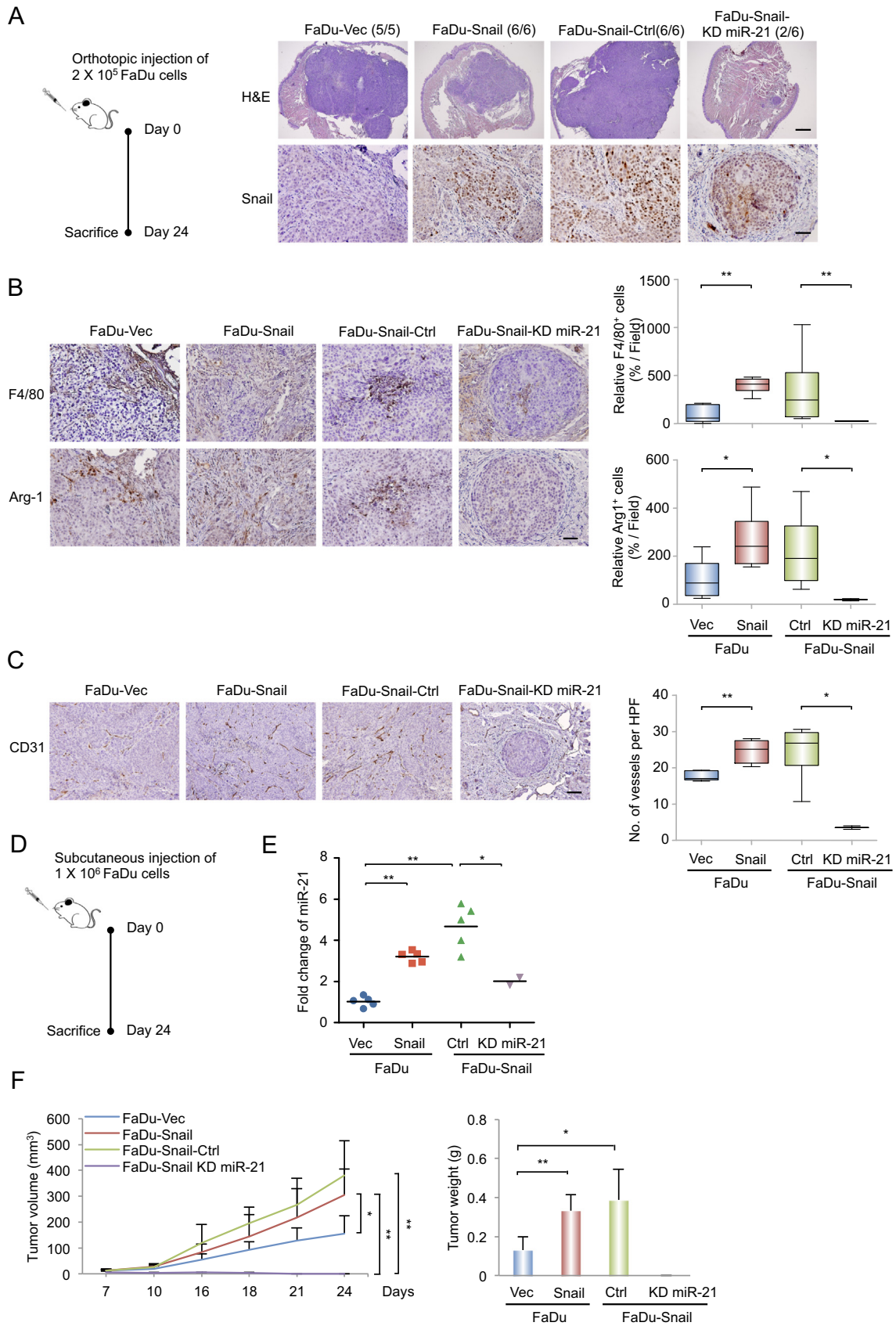
IL-12 (D1200, R&D Systems, Inc., Minneapolis, MN) according to the manufacturer's protocol.

HUVECs Tube Formation Assay

First, 5×10^4 HUVECs were suspended and added into the Matrigel-media 1:1 mixture. The plate was incubated overnight at 37 °C. The images were captured using an inverted microscope (Olympus CKX41, Olympus Corporation, Tokyo, Japan). After 48 hr., tube formation was analyzed and quantified by measuring the number of branches.

Chromatin Immunoprecipitation Assay

For chromatin immunoprecipitation (ChIP) assays, chromosomal DNA fragments were prepared according to the manufacturer's instructions (Thermo Scientific Pierce™ Magnetic ChIP Kit, Waltham, MA). The lysates were incubated with an anti-Snail, and IgG served as a control for immunoprecipitation. The regions concerned were amplified by quantitative PCR.

Luciferase Reporter Assay

For the *MIR21* promoter reporter assay, 50 ng of the wild-type or mutated reporter constructs, 100 ng of the internal control plasmid pCMV-β-gal, and 3 μg of pCDH-Snail or empty vector were co-transfected into HEK293T cells. The luciferase activity was measured after 48 hr.

Immunohistochemistry Assay

The paraffin-embedded tissue sections were deparaffinized, retrieved, washed with water and blocked with 3% hydrogen peroxide. The samples were washed first with water and then with PBS, after which they were blocked and stained with antibodies and then subjected to enzymatic Avidin-Biotin Complex (ABC)-diaminobenzidine (DAB) staining (Leica Biosystems, Wetzlar, Germany). The nuclei were counterstained with hematoxylin. All comparative images were obtained using identical microscope and camera settings (Olympus BX51, Olympus Corporation, Tokyo, Japan). ImageJ software was used for computerized quantification of immunostained F4/80- and arginase-1-positive cells. Microvascular density (MVD) was determined by staining for CD31, an endothelial cell marker, in the tumor samples and by counting all vessels at 400x magnification. Each stained lumen was regarded as a single countable microvessel. Values are expressed as the number of vessels/high-power field.

Patient Samples

The study was approved by the Institutional Review Board of Taipei Veterans General Hospital (TVGH-IRB certificate No. 2014–03-004 AC). The frozen samples of paired tumors and contralateral normal oral epithelia were obtained from 38 HNSCC patients who received treatment at Taipei Veterans General Hospital (Figure 6A-B and Supplementary Figure 5). The relative expression of *SNAI1* and *MRC1* was determined by analyzing the fold changes in tumor tissues from normal counterparts. Patient characteristics of the HNSCC samples are listed in Supplementary Table 1.

Reagents

Proteinase K (Cat. No. P4850) was purchased from Sigma (Sigma-Aldrich, Inc., St. Louis, MO). Recombinant human M-CSF (Cat. No. 300–25) and GM-CSF (Cat. No. 300–03) were purchased from PeproTech Asia (PeproTech, Inc., Rocky Hill, NJ). The Matrigel (Cat. No. 354234) was purchased from BD (BD Transduction Laboratories™, Franklin Lakes, NJ).

Statistics

Two-tailed independent Student's t-test was used to compare the continuous variables between two groups. All statistical data were derived from at least three independent biological replicates, and each experiment contained at least two technical replicates. P values ≤.05 were considered to be significant.

Results

Snail-Expressing Cancer Cells Promote M2-like Polarization of Macrophages

We previously showed that Snail-expressing cancer cells recruit TAMs by secreting cytokines such as CCL2, CCL5, and IL-8 [22]. However, the direct impact of Snail expression on the polarity of TAMs is unclear. Here, we investigated the influence of Snail-expressing cancer cells on the polarization of TAMs. We collected the conditioned media from the HNSCC cell line FaDu with ectopic expression of Snail (FaDu-Snail) or a control vector (FaDu-Vec). The EMT changes of FaDu-Snail was validated by examining the expression of epithelial markers (E-cadherin and γ-catenin) and mesenchymal markers (N-cadherin and vimentin) (Supplementary Figure 1). Freshly isolated CD14$^+$ PBMCs were incubated with FaDu-Snail/FaDu-Vec conditioned media for 48 hr. (Figure 1A). The conditioned media from the FaDu-Snail cells but not from the control cells decreased the expression of M1 markers (*IL18*, *IL12B*, and *HLADR*) and increased the expression of M2 markers (*MRC1*, *CD163*, and *IL10*) in CD14$^+$ monocytes (Figure 1B). Because cytokines are considered the major component in conditioned media, we examined the effect of the major cytokines from the Snail-expressing cells on macrophage polarization. However, the cytokines upregulated in FaDu-Snail were not the canonical M2-polarizing cytokines (Figure 1C). Furthermore, the major M2-polarizing cytokines IL-4 and IL-10 were not increased in the conditioned

Figure 5. miR-21 inhibition suppresses snail induced M2-like macrophages polarization and tumor progression. (A) Left, schema for animal experiment. 2×10^5 FaDu cells were inoculated into the tongue of the nude mice (FaDu-Vec group, n = 5; other groups, n = 6) and were sacrificed at the 24th day. Right, H&E stain and immunohistochemical (IHC) staining of Snail in orthotopic tumors. Scale bar, 1 mm (H&E) and 50 μm (Snail). (B) Left, IHC staining of F4/80 and arginase-1 for showing the recruitment of macrophages in FaDu-formed tumors. Right, quantification of F4/80 and arginase-1 positive cells in orthotopic tumors. The result is present as the fold change of the percentage of F4/80 or arginase-1 positive macrophages in tumor. Scale bar, 50 μm. Data represent means ± S.D. * P < .05, ** P < .005 by Student's t-test. (C) Left, IHC staining of CD31 in orthotopic tumors. Right, quantification of the vessels per high power field (HPF). Scale bar, 100 μm. Data represent means ± S.D. * P < .05, ** P < .005 by Student's t-test. (D) Schema for the animal experiment in (E). 1×10^6 FaDu cells were inoculated into the subcutaneous region of the nude mice (n = 5 for each group) and were sacrificed at the 24th day. (E) RT-qPCR for analyzing the expression level of miR-21 in CD11b$^+$F4/80$^+$ macrophages isolated from FaDu-formed tumors. Data represent means ± S.D. * P < .05, ** P < .005 by Student's t-test. (F) The tumor volume (left) and tumor weight (right) of FaDu-formed tumors. Data represent means ± S.D. * P < .05, ** P < .005 by Student's t-test.
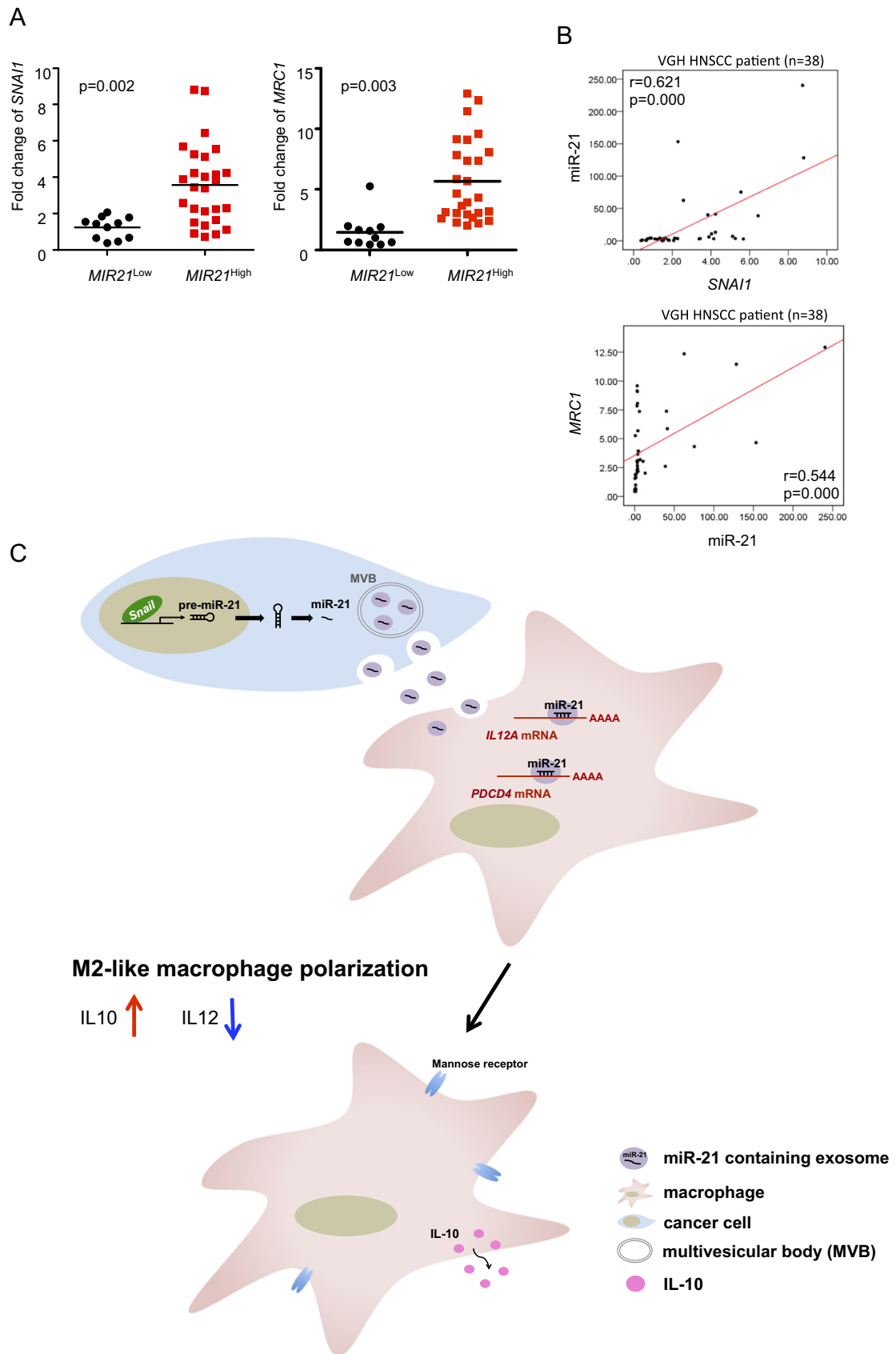
media from FaDu-Snail compared with that from the control cells (Figure 1D). Together, these results indicate that Snail-expressing cancer cells promote M2-like polarization of macrophages.

Purification and Characterization of Tumor-Derived Exosomes

TEXs have been shown to play a pivotal role in tumor-induced immunosuppression, angiogenesis, and pre-metastatic niche formation [25, 26]. Because the cytokines secreted by the Snail-expressing cancer cells were unable to explain the effect of conditional-media-mediated M2 polarization of macrophages, we examined the role of TEXs in TAM polarity. The TEXs were purified by differential ultracentrifugation and confirmed via direct visualization by transmission electron microscopy (TEM) and dynamic light scattering (DLS), which showed the bilayer-membrane nanovesicles with a 50–150 nm diameter (Figure 2A and B). The markers of exosomes, including CD63, CD81, and Alix, were examined to confirm the successful purification of the TEX (Figure 2C). We confirmed the engulfment of TEXs by macrophages via incubation of FaDu cells with PKH26-labeled TEXs and examined the engulfment by fluorescent microscopy and flow cytometry. The PKH26-labeled TEXs were engulfed by PBMC-derived macrophages when co-incubated for 24 hr (Figure 2D and E), suggesting the potential of TEXs in transducing the signals to TAM in tumor tissues.

Exosomes Secreted by Snail-Expressing Cancer Cells Promote M2-Like Polarization of Macrophages

Next, we investigated the impact of TEX on macrophage polarization. CD14$^+$ monocytes were co-incubated with the exosomes from FaDu-Snail compared with those from FaDu-Vec (Figure 3A). RT-qPCR showed that downregulation of the expression of M1 markers (*IL18*, *IL12B*, and *HLADR*) and upregulation of M2 markers (*MRC1*, *CD163*, and *IL10*) in CD14$^+$ monocytes incubated with the exosomes from FaDu-Snail compared with those from FaDu-Vec (Supplemental Figure 2A). Flow cytometry validated the increased surface M2 markers (MR and CD163) and reduced M1 markers (HLA-DR and CD86) in FaDu-Snail-derived TEXs treated monocytes compared with the control ones (Figure 3B). Furthermore, we confirmed the effect of TEXs on regulating TAM polarization in Snail-knockdown OEC-M1 cells vs. control cells. The EMT status of OEC-M1 receiving a shRNA against Snail vs. a control sequence was confirmed (Supplementary Figure 2B). Knocking down Snail in OEC-M1 cells increased the expression of M1 markers (HLA-DR and CD86) and decreased M2 markers (MR and CD163)(Figure 3B). A consistent result was demonstrated when the CD14$^+$ monocytes were treated with the FaDu-Snail-derived exosomes mixed with exosome-free supernatants from the FaDu-control cells (Figure 3C, D and Supplemental Figure 2C), which confirms the role of exosomes from Snail-expressing cancer cells in promoting M2-like polarization. Furthermore, treatment of the GM-CSF-primed macrophages with the exosomes from FaDu-Snail downregulated M1 markers (*HLADR*) and upregulated M2 markers

(*MRC1*/mannose receptor) (Supplementary Figure 2D-F). We next confirmed the function of TEX-polarized macrophages. The level of exosome-loaded cytokines was very low compared with the level of macrophage-secreted cytokines (Supplementary Figure 2G), suggesting that the effect of exosome-loaded cytokines may be negligible. Increased IL-10 and reduced IL-12 secretion were noted in monocytes treated with FaDu-Snail exosomes (Figure 3E). An in vitro tube formation assay showed that the pro-angiogenic ability of the CD14$^+$ monocytes was elevated after treatment with the exosomes from FaDu-Snail (Figure 3F). Together, the above results suggest that exosomes from Snail-expressing cancer cells promote M2-like polarization of macrophages.

The Snail-Driven miR-21-Containing TEXs Induce M2-Like Polarization of Macrophages

MiR-21 has been shown to be upregulated in different types of cancers [27, 28], and exosomal miR-21 is noted as a potential biomarker of cancer [29]. The major target of miR-21, programmed cell death protein 4 (PDCD4), which is a tumor suppressor that inhibits protein synthesis [30], has been shown to be directly repressed by miR-21 [31]. Additionally, IL12A has been shown to be repressed by miR-21 [32]. Interestingly, suppression of PDCD4 or IL12A both result in M2 polarization of macrophages [33,34]. Because miR-21 is an important cancer-associated microRNA, and miR-21-containing TEX promote M2 polarization of macrophages, we assumed that miR-21 is the key molecule in Snail-derived TEX for M2 polarization. We first examined the expression of miR-21 in GM-CSF- or M-CSF-primed macrophages, which indicate pro-inflammatory and anti-inflammatory macrophages, respectively [35]. An increased level of miR-21 was observed in M-CSF macrophages compared with the GM-CSF macrophages (Figure 4A), indicating the abundancy of miR-21 in anti-inflammatory macrophages. Treatment of the CD14$^+$ monocytes with exosomes derived from FaDu-Snail demonstrated upregulation of miR-21 (Figure 4B). Upregulation of miR-21 and downregulation of the miR-21 target *PDCD4* and *IL12A* were observed when the GM-CSF-primed macrophages were incubated with the FaDu-Snail-derived exosomes (Supplementary Figure 3). A more significant reduction of miR-21 was observed in the exosomes treated with both Triton X-100/proteinase K and RNase A compared with other groups, suggesting that miR-21 indeed exists in TEX (Figure 4C).

We next explored the mechanism of miR-21 upregulation by Snail. Overexpression of Snail in the FaDu cells increased miR-21 expression, whereas knockdown of Snail in the HNSCC line OEC-M1 significantly reduced miR-21 (Figure 4D). The chromatin immunoprecipitation assay confirmed the direct binding of Snail to the proximal promoter of *MIR21* under TGF-β treatment (Figure 4E). The reporter assay showed that Snail increases the activity of the *MIR21* promoter through specific E-box binding motif, and mutation or deletion of the binding sites abrogated the Snail-induced promoter activation (Figure 4F). Together, these

Figure 6. miR-21 correlates with the expression of M2 markers in head and neck cancers. (A) RT-qPCR for analyzing the expression level of miR-21, *SNAI1*, and the M2 marker *MRC1* in HNSCC samples. n = 38. The miR-21^{High} (n = 27) is defined as the level higher than mean value, and the miR-21^{Low} (n = 11) is defined as the level lower than mean value. The p value is shown in each panel. (B) Scatter plot for showing the correlation between the level of *SNAI1* and miR-21 (upper panel) as well as *MRC1* and miR-21 (lower panel) in 38 patients with HNSCC. The p value and correlation coefficient r are shown in each panel. (C) A proposed model for cancer-derived miR-21 containing exosomes in regulating M2-like macrophages polarization. In cancer cells (blue), Snail activates the transcription of *MIR21* and increase the secretion of miR-21-containing exosomes; MVB, multivesicular bodies. In macrophages (pink), miR-21 suppresses the expression of the target genes (e.g., *PDCD4*, *IL12A*) to promote M2 polarization.

results indicate that in Snail-overexpressing cancer cells, direct activation of *MIR21* transcription by Snail increases miR-21 production. An enrichment of miR-21 in the TEXs downregulated PDCD4 and IL12A in macrophages, mediating M2 polarization.

Snail-Regulated miR-21 Modulates M2-Like Polarization of TAMs and Promotes Tumor Progression in vivo and in Patient Samples

We next confirmed the role of Snail-regulated miR-21 in TAM polarization and tumor progression *in vivo*. First, we designed an experiment to confirm the successful delivery of miR-21 to TAMs through exosomes. We ectopically expressed CD81, an exosomal marker, in the FaDu-Snail/FaDu-Vec cells (Supplementary Figure 4A). The cells were inoculated in the nude mice, and the xenograft tumors were harvested on the 14th day (Supplementary Figure 4B). Flow cytometry analysis was performed to sort the F4/80$^+$ TAMs for analyzing the expression of Flag-tagged CD81 in the TAMs. The TEXs from either FaDu-Snail or FaDu-Vec were internalized by the TAMs (Supplementary Figure 4C). We next confirmed the effect of Snail-regulated miR-21 on TAM polarization and tumor progression. Knockdown of miR-21 or a scrambled control sequence was performed in the FaDu-Snail cells (Supplementary Figure 4D), and the level of miR-21 in corresponding sublines were validated (Supplementary Figure 4E). We inoculated these cells into the nude mice to investigate the effect of Snail-regulated miR-21 on TAM polarization and tumor progression. The mice were sacrificed, and the xenograft tumors were harvested on the 24th day (Figure 5A). For TAM polarity, the FaDu-Snail-formed tumors were infiltrated with TAM expressing a high level of M2 markers compared with that of the FaDu-Vec control cells. Knockdown of miR-21 in FaDu-Snail reduced M2 infiltration and microvascular density in tumors (Figure 5B and C).

We next evaluated the impact of Snail-regulated miR-21 on tumor growth (Figure 5D). Firstly, we confirmed the expression of miR-21 in F4/80$^+$CD11b$^+$ TAMs sorted from the tumors formed by corresponding sublines (FaDu-Vec, FaDu-Snail, FaDu-Snail-KD-miR21, and FaDu-Snail-KD-control). The TAM isolated from FaDu-Snail-formed tumor expressing a higher level of miR-21 than TAMs from FaDu-Vec-formed tumors, and knockdown of miR-21 in FaDu-Snail suppressed miR-21 expression in TAMs (Figure 5E). For tumor progression, the FaDu-Snail-formed tumors exhibited an increased tumor weight and tumor volume, and knockdown of miR-21 in FaDu-Snail attenuated the Snail-mediated tumor progression (Figure 5F).

Finally, we confirmed the above observations in patient samples. Thirty-eight HNSCC patient samples were collected to examine the expression of *SNAI1*, miR-21, and the M2 marker *MRC1*. Among them, HPV status were available in 12 cases. An increased level of *SNAI1* as well as the M2 marker *MRC1* was observed in the samples with a higher expression of miR-21 (Figure 6A). A positive correlation between the expression of *SNAI1* and miR-21 as well as *MRC1* and miR-21 were demonstrated in 38 HNSCC samples (Figure 6B). In the HPV status-available cases, there was no significant difference in the expression of *SNAI1*, *MRC1*, and miR-21 among the HPV(+) group vs. HPV(–) group (Supplementary Figure 5).

We propose a model to summarize our observations in this study in Figure 6C. The Snail-expressing tumor cells secrete miR-21-abundant TEXs, which polarize the TAMs to a M2-like phenotype by targeting *PDCD4* and *IL12A*. Mechanistically, Snail activates the

transcription of *MIR21* through direct binding to the promoter. The miR-21-mediated M2 polarization of the TAMs contributes to the Snail-mediated cancer progression.

Discussion

The role of TEXs in remodeling the TME has been extensively investigated recently. TEXs carry a cargo of molecules and deliver them to recipient cells for serving as a communication network between cancer cells and microenvironments. Because exosomes are considered to reflect the status and identity of the parent cells [36], the cargo transferred to the recipient cells may be closely related to their expression levels in parental cancer cells. Accumulating evidence supports the oncogenic roles of miR-21 in human cancer. MiR-21 is frequently overexpressed in different types of human cancers, including non-small cell lung cancers, HNSCC and breast cancer. [37-39]. Plasma miR-21 has been reported to be a candidate biomarker in colorectal cancer [40], as well as gastric cancer [41]. In the current study, we show that increased production of miR-21 in HNSCC results in the generation of miR-21-abundant TEXs, which transfer miR-21 to the TAMs to modulate their polarization and activity. This observation extends the understanding of the oncogenic role of miR-21 beyond the well-established intracellular signaling of miR-21: oncogenic miR-21 affects not only cancer cells but also host immune cells. Importantly, we confirmed the positive association between miR-21 and *SNAI1/MRC1* in HNSCC samples, suggesting the potential of miR-21 as a biomarker for reflecting the status of the TME. Immuno-oncology (IO) has been the state-of-the-art treatment of advanced HNSCC [42]; however, the biomarkers are lacking for selecting the optimal patient population and monitoring treatment responses. Application of miR-21 as the guide for tailoring immunotherapies and dynamically reflecting the status of the TME in patients under IO treatment in advanced HNSCC is potentially an attractive strategy and requires extensive clinical investigation.

Considering the major mechanism of miR-21-mediated oncogenic effects, miR-21 inhibits the expression of a variety of tumor suppressors such as *PTEN* [43], *PDCD4* [31,44] and *IGFBP3* [45] through direct binding to the 3'-UTR of target transcripts. Regarding the inducing signals of miR-21, previous studies suggest that NF-κB and STAT3 pathways are the major upstream pathways of miR-21 in monocytes/macrophages, as well as fibroblasts [46]. However, the pathways responsible for the generation of oncogenic miR-21 in cancer cells is relatively unclear. In this work, we show that the EMT-TF Snail induces the expression of miR-21 in cancer cells, leading to the secretion of miR-21-abundant TEXs to promote M2 polarization of TAMs. Since the major input signals for EMT induction in cancer cells have been well-established [20,21], the mechanisms underlying the production of miR-21-abundant TEXs is clear. Additionally, miR-21 has been observed to induce EMT [47,48]. This result, together with our findings, suggests that in cancer cells, miR-21 and EMT form a positive feedback loop to amplify the signal; these cancer cells produce miR-21-abundant TEX to transmit the signals to the TME for further facilitation of tumor progression. An open question in this study is whether Snail is the only EMT-TF responsible for producing miR-21-containing TEX, because the Snail-binding motifs of *MIR21* may also be activated by other EMT-TFs harboring the same binding sequences, such as Slug and Twist1. Further investigation is required to elucidate the role of different EMT-TFs in activating *MIR21* transcription and producing miR-21-containing TEX.

Increasing evidence supports miRNAs as the major players in the signal network of EMT, and deregulation of certain miRNAs has been considered the hallmark of EMT [49]. MiR-200 family microRNAs are the major epithelial markers [50]. The miR-200 family formed a feedback loop with ZEB1/ZEB2 to regulate EMT [51,52]. The EMT-TF Twist1 induced the expression of miR-10b, which suppressed HOXD10 to increase cell motility and cancer invasion [53]. We previously showed that Twist1 cooperates with BMI1 to suppress let-7i expression in HNSCC [54]. In colon cancer stem cells, Snail regulates the expression of miR-146a to induce symmetrical division for expanding stem cell pool and malignant progression [55]. Since miRNA deregulation is a major consequence of EMT-TF activation, the role of other miRNAs needs to be further explored in TEXs secreted by cells undergoing EMT in cancer progression.

In conclusion, our findings elucidate the tumor-macrophage interplay through communication with exosomes during EMT. The major clinical impact of the current study relies on two rationales. First, exosomal miRNAs are relatively easy to detect and quantify compared to the oncogenic proteins in tumor cells, which may greatly extend their application. Second, exosomal miR-21 may not only serve as a biomarker of tumor progression but also indicate the real-time situation in the TME, which will be very valuable for optimizing cancer immunotherapies.

Disclosure of Potential Conflicts of Interests

The authors declare that no competing financial interests exist with this study.

Acknowledgments

Appendix A. Supplementary Data

Supplementary data to this article can be found online at https://doi.org/10.1016/j.neo.2018.06.004.

References

[1] Gajewski TF, Schreiber H, and Fu YX (2013). Innate and adaptive immune cells in the tumor microenvironment. *Nat Immunol* **14**, 1014–1022.

[2] Galdiero MR, Bonavita E, Barajon I, Garlanda C, Mantovani A, and Jaillon S (2013). Tumor associated macrophages and neutrophils in cancer. *Immunobiology* **218**, 1402–1410.

[3] Murray PJ, Allen JE, Biswas SK, Fisher EA, Gilroy DW, Goerdt S, Gordon S, Hamilton JA, Ivashkiv LB, and Lawrence T, et al (2014). Macrophage activation and polarization: nomenclature and experimental guidelines. *Immunity* **41**, 14–20.

[4] Gordon S and Martinez FO (2010). Alternative activation of macrophages: mechanism and functions. *Immunity* **32**, 593–604.

[5] Qian BZ and Pollard JW (2010). Macrophage diversity enhances tumor progression and metastasis. *Cell* **141**, 39–51.

[6] Mantovani A, Sozzani S, Locati M, Allavena P, and Sica A (2002). Macrophage polarization: tumor-associated macrophages as a paradigm for polarized M2 mononuclear phagocytes. *Trends Immunol* **23**, 549–555.

[7] Liao D, Luo Y, Markowitz D, Xiang R, and Reisfeld RA (2009). Cancer associated fibroblasts promote tumor growth and metastasis by modulating the tumor immune microenvironment in a 4T1 murine breast cancer model. *PLoS One* **4**e7965.

[8] Tiemessen MM, Jagger AL, Evans HG, van Herwijnen MJ, John S, and Taams LS (2007). CD4+CD25+Foxp3+ regulatory T cells induce alternative activation of human monocytes/macrophages. *Proc Natl Acad Sci U S A* **104**, 19446–19451.

[9] Wang H, Shao Q, Sun J, Ma C, Gao W, Wang Q, Zhao L, and Qu X (2016). Interactions between colon cancer cells and tumor-infiltrated macrophages depending on cancer cell-derived colony stimulating factor 1. *Oncoimmunology* **5**e1122157.

[10] Zhang HG and Grizzle WE (2014). Exosomes: a novel pathway of local anddistant intercellular communication that facilitates the growth and metastasis of neoplastic lesions. *Am J Pathol* **184**, 28–41.

[11] Thery C, Ostrowski M, and Segura E (2009). Membrane vesicles as conveyors of immune responses. *Nat Rev Immunol* **9**, 581–593.

[12] Choi DS, Kim DK, Kim YK, and Gho YS (2013). Proteomics, transcriptomics and lipidomics of exosomes and ectosomes. *Proteomics* **13**, 1554–1571.

[13] Valadi H, Ekstrom K, Bossios A, Sjostrand M, Lee JJ, and Lotvall JO (2007). Exosome-mediated transfer of mRNAs and microRNAs is a novel mechanism of genetic exchange between cells. *Nat Cell Biol* **9**, 654–659.

[14] Skog J, Wurdinger T, van Rijn S, Meijer DH, Gainche L, Sena-Esteves M, Curry Jr WT, Carter BS, Krichevsky AM, and Breakefield XO (2008). Glioblastoma microvesicles transport RNA and proteins that promote tumour growth and provide diagnostic biomarkers. *Nat Cell Biol* **10**, 1470–1476.

[15] Andreola G, Rivoltini L, Castelli C, Huber V, Perego D, Deho P, Squarcina P, Accornero P, Lozupone F, and Lugini L, et al (2002). Induction of lymphocyte apoptosis by tumor cell secretion of FasL-bearing microvesicles. *J Exp Med* **195**, 1303–1316.

[16] Clayton A, Mitchell JP, Court J, Mason MD, and Tabi Z (2007). Human tumor-derived exosomes selectively impair lymphocyte responses to interleukin-2. *Cancer Res* **67**, 7458–7466.

[17] Kucharzewska P, Christianson HC, Welch JE, Svensson KJ, Fredlund E, Ringner M, Morgelin M, Bourseau-Guilmain E, Bengzon J, and Belting M (2013). Exosomes reflect the hypoxic status of glioma cells and mediate hypoxiadependent activation of vascular cells during tumor development. *Proc Natl Acad Sci U S A* **110**, 7312–7317.

[18] Costa-Silva B, Aiello NM, Ocean AJ, Singh S, Zhang H, Thakur BK, Becker A, Hoshino A, Mark MT, and Molina H, et al (2015). Pancreatic cancer exosomes initiate pre-metastatic niche formation in the liver. *Nat Cell Biol* **17**, 816–826.

[19] Melo SA, Sugimoto H, O'Connell JT, Kato N, Villanueva A, Vidal A, Qiu L, Vitkin E, Perelman LT, and Melo CA, et al (2014). Cancer exosomes perform cell-independent microRNA biogenesis and promote tumorigenesis. *Cancer Cell* **26**, 707–721.

[20] Thiery JP, Acloque H, Huang RY, and Nieto MA (2009). Epithelial-mesenchymal transitions in development and disease. *Cell* **139**, 871–890.

[21] Kalluri R and Weinberg RA (2009). The basics of epithelial-mesenchymal transition. *J Clin Invest* **119**, 1420–1428.

[22] Hsu DS, Wang HJ, Tai SK, Chou CH, Hsieh CH, Chiu PH, Chen NJ, and Yang MH (2014). Acetylation of snail modulates the cytokinome of cancer cells to enhance the recruitment of macrophages. *Cancer Cell* **26**, 534–548.

[23] Huang YH, Lin YH, Chi HC, Liao CH, Liao CJ, Wu SM, Chen CY, Tseng YH, Tsai CY, and Lin SY, et al (2013). Thyroid hormone regulation of miR-21 enhances migration and invasion of hepatoma. *Cancer Res* **73**, 2505–2517.

[24] Thery C, Amigorena S, Raposo G, and Clayton A (2006). Isolation and characterization of exosomes from cell culture supernatants and biological fluids. *Curr Protoc Cell Biol* **3**(22). doi:10.1002/0471143030.cb0322s30.

[25] Peinado H, Aleckovic M, Lavotshkin S, Matei I, Costa-Silva B, Moreno-Bueno G, Hergueta-Redondo M, Williams C, Garcia-Santos G, and Ghajar C, et al (2012). Melanoma exosomes educate bone marrow progenitor cells toward a pro-metastatic phenotype through MET. *Nat Med* **18**, 883–891.

[26] Zhou W, Fong MY, Min Y, Somlo G, Liu L, Palomares MR, Yu Y, Chow A, O'Connor ST, and Chin AR, et al (2014). Cancer-secreted miR-105 destroys vascular endothelial barriers to promote metastasis. *Cancer Cell* **25**, 501–515.

[27] Hatley ME, Patrick DM, Garcia MR, Richardson JA, Bassel-Duby R, van Rooij E, and Olson EN (2010). Modulation of K-Ras-dependent lung tumorigenesis by MicroRNA-21. *Cancer Cell* **18**, 282–293.

[28] Medina PP, Nolde M, and Slack FJ (2010). OncomiR addiction in an in vivo model of microRNA-21-induced pre-B-cell lymphoma. *Nature* **467**, 86–90.

[29] Zhao J, Zhang Y, and Zhao G (2015). Emerging role of microRNA-21 in colorectal cancer. *Cancer Biomark* **15**, 219–226.

[30] Cmarik JL, Min H, Hegamyer G, Zhan S, Kulesz-Martin M, Yoshinaga H, Matsuhashi S, and Colburn NH (1999). Differentially expressed protein Pdcd4 inhibits tumor promoter-induced neoplastic transformation. *Proc Natl Acad Sci U S A* **96**, 14037–14042.

[31] Asangani IA, Rasheed SA, Nikolova DA, Leupold JH, Colburn NH, Post S, and Allgayer H (2008). MicroRNA-21 (miR-21) post-transcriptionally down-regulates tumor suppressor Pdcd4 and stimulates invasion, intravasation and metastasis in colorectal cancer. *Oncogene* **27**, 2128–2136.

[32] Lu TX, Munitz A, and Rothenberg ME (2009). MicroRNA-21 is up-regulated in allergic airway inflammation and regulates IL-12p35 expression. *J Immunol* **182**, 4994–5002.

[33] Sheedy FJ, Palsson-McDermott E, Hennessy EJ, Martin C, O'Leary JJ, Ruan Q, Johnson DS, Chen Y, and O'Neill LA (2010). Negative regulation of TLR4 via targeting of the proinflammatory tumor suppressor PDCD4 by the microRNA miR-21. *Nat Immunol* **11**, 141–147.

[34] Kan X, Wu Y, Ma Y, Zhang C, Li P, Wu L, Zhang S, Li Y, and Du J (2016). Deficiency of IL-12p35 improves cardiac repair after myocardial infarction by promoting angiogenesis. *Cardiovasc Res* **109**, 249–259.

[35] Lacey DC, Achuthan A, Fleetwood AJ, Dinh H, Roiniotis J, Scholz GM, Chang MW, Beckman SK, Cook AD, and Hamilton JA (2012). Defining GM-CSF- and macrophage-CSF-dependent macrophage responses by in vitro models. *J Immunol* **188**, 5752–5765.

[36] Kunigelis KE and Graner MW (2015). The dichotomy of tumor exosomes (TEX) in cancer immunity: Is It All in the ConTEXt? *Vaccines (Basel)* **3**, 1019–1051.

[37] Niu J, Shi Y, Tan G, Yang CH, Fan M, Pfeffer LM, and Wu ZH (2012). DNA damage induces NF-kappaB-dependent microRNA-21 up-regulation and promotes breast cancer cell invasion. *J Biol Chem* **287**, 21783–21795.

[38] Liu ZL, Wang H, Liu J, and Wang ZX (2013). MicroRNA-21 (miR-21) expression promotes growth, metastasis, and chemo- or radioresistance in non-small cell lung cancer cells by targeting PTEN. *Mol Cell Biochem* **372**, 35–45.

[39] Mydlarz W, Uemura M, Ahn S, Hennessey P, Chang S, Demokan S, Sun W, Shao C, Bishop J, and Krosting J, et al (2014). Clusterin is a gene-specific target of microRNA-21 in head and neck squamous cell carcinoma. *Clin Cancer Res* **20**, 868–877.

[40] Kanaan Z, Rai SN, Eichenberger MR, Roberts H, Keskey B, Pan J, and Galandiuk S (2012). Plasma miR-21: a potential diagnostic marker of colorectal cancer. *Ann Surg* **256**, 544–551.

[41] Komatsu S, Ichikawa D, Tsujiura M, Konishi H, Takeshita H, Nagata H, Kawaguchi T, Hirajima S, Arita T, and Shiozaki A, et al (2013). Prognostic impact of circulating miR-21 in the plasma of patients with gastric carcinoma. *Anticancer Res* **33**, 271–276.

[42] Ferris RL, Blumenschein Jr G, Fayette J, Guigay J, Colevas AD, Licitra L, Harrington K, Kasper S, Vokes EE, and Even C, et al (2016). Nivolumab for Recurrent Squamous-Cell Carcinoma of the Head and Neck. *N Engl J Med* **375**, 1856–1867.

[43] Meng F, Henson R, Wehbe-Janek H, Ghoshal K, Jacob ST, and Patel T (2007). MicroRNA-21 regulates expression of the PTEN tumor suppressor gene in human hepatocellular cancer. *Gastroenterology* **133**, 647–658.

[44] Frankel LB, Christoffersen NR, Jacobsen A, Lindow M, Krogh A, and Lund AH (2008). Programmed cell death 4 (PDCD4) is an important functional target of the microRNA miR-21 in breast cancer cells. *J Biol Chem* **283**, 1026–1033.

[45] Yang CH, Yue J, Pfeffer SR, Fan M, Paulus E, Hosni-Ahmed A, Sims M, Qayyum S, Davidoff AM, and Handorf CR, et al (2014). MicroRNA-21 promotes glioblastoma tumorigenesis by down-regulating insulin-like growth factor-binding protein-3 (IGFBP3). *J Biol Chem* **289**, 25079–25087.

[46] Yang CH, Yue J, Fan M, and Pfeffer LM (2010). IFN induces miR-21 through a signal transducer and activator of transcription 3-dependent pathway as a suppressive negative feedback on IFN-induced apoptosis. *Cancer Res* **70**, 8108–8116.

[47] Liu W, Zhang B, Chen G, Wu W, Zhou L, Shi Y, Zeng Q, Li Y, Sun Y, and Deng X, et al (2017). Targeting miR-21 with Sophocarpine Inhibits Tumor Progression and Reverses Epithelial-Mesenchymal Transition in Head and Neck Cancer. *Mol Ther* **25**, 2129–2139.

[48] Liu Z, Jin ZY, Liu CH, Xie F, Lin XS, and Huang Q (2015). MicroRNA-21 regulates biological behavior by inducing EMT in human cholangiocarcinoma. *Int J Clin Exp Pathol* **8**, 4684–4694.

[49] Nicoloso MS, Spizzo R, Shimizu M, Rossi S, and Calin GA (2009). MicroRNAs–the micro steering wheel of tumour metastases. *Nat Rev Cancer* **9**, 293–302.

[50] Gibbons DL, Lin W, Creighton CJ, Rizvi ZH, Gregory PA, Goodall GJ, Thilaganathan N, Du L, Zhang Y, and Pertsemlidis A, et al (2009). Contextual extracellular cues promote tumor cell EMT and metastasis by regulating miR-200 family expression. *Genes Dev* **23**, 2140–2151.

[51] Gregory PA, Bert AG, Paterson EL, Barry SC, Tsykin A, Farshid G, Vadas MA, Khew-Goodall Y, and Goodall GJ (2008). The miR-200 family and miR-205 regulate epithelial to mesenchymal transition by targeting ZEB1 and SIP1. *Nat Cell Biol* **10**, 593–601.

[52] Park SM, Gaur AB, Lengyel E, and Peter ME (2008). The miR-200 family determines the epithelial phenotype of cancer cells by targeting the E-cadherin repressors ZEB1 and ZEB2. *Genes Dev* **22**, 894–907.

[53] Ma L, Teruya-Feldstein J, and Weinberg RA (2007). Tumour invasion and metastasis initiated by microRNA-10b in breast cancer. *Nature* **449**, 682–688.

[54] Yang WH, Lan HY, Huang CH, Tai SK, Tzeng CH, Kao SY, Wu KJ, Hung MC, and Yang MH (2012). RAC1 activation mediates Twist1-induced cancer cell migration. *Nat Cell Biol* **14**, 366–374.

[55] Hwang WL, Jiang JK, Yang SH, Huang TS, Lan HY, Teng HW, Yang CY, Tsai YP, Lin CH, and Wang HW, et al (2014). MicroRNA-146a directs the symmetric division of Snail-dominant colorectal cancer stem cells. *Nat Cell Biol* **16**, 268–280.